

# **The 28 December 1908, Messina Straits earthquake ( $M_w$ 7.1): A great earthquake through a century of seismology**

Nicola Alessandro Pino, Alessio Piatanesi, Gianluca Valensise and Enzo Boschi

*Istituto Nazionale di Geofisica e Vulcanologia, Italy*

## **Abstract**

The  $M_w$  7.1, 28 December 1908, Messina Straits earthquake has been the deadliest earthquake in recent European history and also one of the first to be investigated with modern instrumental data. Throughout a full century, in parallel with the evolution of seismology as a research discipline, scientists from all over the world confronted the complexity and elusiveness of its source and the diversity of its effects on buildings and on the environment.

Investigations of the 1908 earthquake went through three distinct phases. In the first phase (1909-late 1970s) all available observations were used to derive the main source parameters with simplified methods, starting with determinations of the epicenter from free-falling bodies. In the second phase (early 1980s) all data were reconsidered with modern methods involving extensive computer modeling, which described the seismic source based largely on the distribution of elevation changes due to the earthquake. In the third phase (since 2000), state-of-the-art seismological approaches (such as waveform modeling, joint inversion of seismological and geodetic data, dating of paleotsunami deposit) are being used to shed light on the more debated aspects of the event, such as the exact origin of the tsunami.

This paper summarizes the full evolutionary path of these investigations, pointing out misconceptions, major achievements and turning points, and discusses the established vs. the debated facts in the understanding of the earthquake causative source.

## 1. Introduction

Early in the morning on 28 December 1908, just a few days after Christmas, a severe earthquake struck the Messina Straits, a rather narrow sound that separates Sicily from Calabria, in southern Italy (**Figure 1**). The shaking was distinctly felt in Albania, Montenegro and the Greek Ionian islands, about 400 km to the east and northeast of the Straits; in Malta, about 250 km to the south; and as far as Ustica Island, about 220 km to the west. The earthquake was catastrophic in the epicentral area and was immediately followed by fires and by a large tsunami. Messina (Sicily) and Reggio Calabria (Calabria), two significant cities located less than 10 km apart on the two facing shores of the Straits, were almost completely destroyed and buildings were severely damaged over an area in excess of 6,000 km<sup>2</sup>. A significant fraction of the population, numbering 140,000 at Messina and 45,000 at Reggio Calabria, was reported dead. Assessing the total number of victims has been problematic, as fatality estimates range from 60,000 to over 100,000, yet 1908 was undeniably the deadliest European earthquake ever and one of the deadliest worldwide. *Guidoboni et al.* [2007] contend that 80,000 people were killed by the earthquake, including as many as 2,000 who died as a result of the tsunami. Waves up to 12 meters struck the shorelines south of Messina and south of Reggio Calabria, completing the destruction and displacing the rubble from collapsed buildings. All communications in the affected area were disrupted, and rescue operations had to rely on access from the sea. Units of the Russian and English navies, already in the area, were the first to offer immediate relief. In particular, medical officers of the Baltic Guard-Marine brought the first medical aid to the earthquake victims, and Russian researchers were the first to offer psychiatric assistance.

Damage in Messina and Reggio Calabria was exacerbated by the poor quality of construction and building materials, as well as by the occurrence of significant earthquakes during the preceding 15 years. Especially in southern Calabria, the population and their dwellings had been shattered in 1894, 1905 and 1907 during earthquakes that were all larger than  $M_e > 6$  ( $M_e$  is an equivalent magnitude obtained from intensity data [Boschi *et al.*, 1995]; **Figure 1**). The Messina Straits locate in the middle of the Calabrian Arc, one of the most seismically active areas of the Italian region and of the entire Mediterranean basin. The Straits area itself had been struck several times in the past, though not with the same violence as in 1908. The historical record [Guidoboni *et al.*, 2007] reports at least three earthquakes with  $M_e > 5.5$ , respectively on 31 August 853 ( $I_0$  IX-X), 25 February 1509 ( $I_0$  VIII), and 6 February 1783 ( $I_0$  VIII-IX). The last event took place at the northern end of the Straits and was part of a 2-month sequence of five major earthquakes that struck a 100 km-long stretch of southern and central Calabria. All these earthquakes had  $I_0$  between VIII-IX and XI and produced extensive damage both in southern Calabria and northeastern Sicily, and particularly in Messina. The historical records also report more elusive but presumably significant earthquakes in 91 B.C. ( $I_0$  IX-X) and 361 A.D. ( $I_0$  X).

After a few decades of great progress in the development of seismological instruments [Dewey and Byerly, 1969], the beginning of the twentieth century witnessed a dramatic increase in the number of seismic instruments installed worldwide, some of which had the latest designs and were rather reliable in their performance. For instance, many Wiechert seismographs were in use around the world in the early 1900's, providing good quality recordings that can still be analyzed with modern techniques. Some of these instruments are still operational (e.g., Göttingen, Sweden [Ritter, 2002]). Besides, due to the simple optical principles underlying the measuring techniques, ground-surface leveling instruments available at the time were nearly as reliable as recent ones.

Despite the fast progress in the number and technological characteristics of the available instruments, however, the cause and mechanism of earthquakes were largely unknown. The existence of a close link between faulting and earthquakes had started to be accepted in the second half of the nineteenth century following observations that earthquake patterns can be related to geographical and geological features [*Hoernes*, 1878] and observations of coseismic surface breaks matching the topography [*Gilbert*, 1884]. These pioneering ideas gained momentum following the major San Francisco earthquake of 18 April 1906. The first report on this earthquake, prepared by a commission chaired by *Lawson* [1908], put together a large set of observations, including surveys on the damage distribution and surface ruptures, seismic recordings from worldwide stations, and geological analyses on the crustal structure of the epicentral region. Taking advantage of these observations, *Reid* [1910] developed the theory of elastic rebound, which was published in the second volume of the Commission report. This effort provided the first unifying picture of the physical process associated with rupture in the Earth's crust.

In such a rapidly changing scientific framework of earthquake theory, many scientists from all over the world went to the Messina Straits area immediately after the 1908 earthquake event and investigated the effects of the ground shaking on buildings and on the natural environment. The origin of the 1908 earthquake itself was largely debated by contemporary scholars: a violent volcanic explosion in the Straits was a popular hypothesis, implying that the great advances in the understanding of the seismic source prompted by investigations of the San Francisco earthquake had evidently not yet become common ground for all seismologists. Such delayed acceptance of the nature of earthquake source physics and the limited computational resources of the time did not allow a thorough analysis and the development of a comprehensive model of the earthquake. Nevertheless, the observations and measurements by the early investigators of the 1908 earthquake

and tsunami formed the basis for a century of analyses and ultimately allowed later scientists to achieve the present knowledge on the earthquake tectonic setting, the geometry, mode and style of its causative rupture, the genesis of the tsunami and the causes of the uneven damage distribution.

## **2. Observations and early studies: at the dawn of quantitative seismology**

The great quantity of observations accumulated by the investigators of the time included extensive field reports on the effects of the earthquake, photographs of damaged buildings, witness accounts of the tsunami wave and of various phenomena associated with the earthquake (rumble, luminescence, etc.), and of course instrumental data (**Table 1**). No surface break that could be directly related with the earthquake fault was reported, but several secondary surface effects were observed both in Sicily and Calabria. Variations in the water level in pools and wells, ground fractures and many landslides and rockfalls were reported over a large area encompassing the intensity X and XI areas. Significant subsidence occurred on both sides of the Straits but particularly along the Calabrian shoreline, where the coast retreated by as much as 70 m. Following is a summary of the observations collected by the early investigators and circulated to the entire scientific community. Although most of the observations were of a qualitative nature, many were obtained from state-of-the-art instrumentation and were, in a sense, much “ahead of their time”.

### **2.1. Macroseismic observations**

The reports by *Mercalli* [1909] and *Omori* [1909] were among the first published on the Messina Straits earthquake. Both described the highly catastrophic consequences of the earthquake and hypothesized that the number of victims was close to 100,000, specifying that the unusual level of destruction was mainly due to the poor quality of the construction, especially in the two main cities destroyed in the earthquake. According to *Baratta* [1910], the severity of the shock induced *Mercalli* to add the XI degree to his own intensity scale, but he also reduced the estimated loss of lives to around 80,000.

At the time of the earthquake many researchers were elaborating intensity scales and methods for deriving earthquake source information from felt report data. Using a method that was developed by *Mallet* [1862] and that was popular during the second half of the nineteenth century, *Omori* [1909] attempted to evaluate what he called the location of the “maximum earthquake motion” from near-field observations of over-turned free-fall bodies, and assumed this to be coincident with the epicenter (**Figure 1**). Besides *Mercalli* [1909] and *Omori* [1909], many scientists published extensive macroseismic studies on the 1908 earthquake. *De Stefani* [1909a], *Martinelli* [1909], *Oddone* [1909], *Perret* [1909] and several others studied the earthquake effects and some of them produced isoseismal maps, but the most complete field survey is that due to *Baratta* [1910]. He collected a considerable amount of very detailed macroseismic data, pointing out the presence of several anomalies in the distribution of the intensity in zones that had already suffered strong damage in the 1783, 1894 and 1905 earthquakes. *Baratta* [1910] related this observation to the presence of areas of “seismic instability”, implicitly suggesting the existence of site amplification effects. Using *Mallet*'s approach with a larger number of observations, he determined a main center corresponding to *Omori*'s epicenter and a second one slightly north of it (**Figure 1**). Determining the epicenter from the arrival times of seismic waves was already common practice, but due to the

difficulties in the determining the correct timing of seismic phases and to the large uncertainties in regional wave propagation models, no attempt was made to this end: the results obtained by *Omori* and *Baratta* were considered reliable enough and indicative of the main seismic center. In fact, none of the numerous scientists who studied the 1908 earthquake in the years immediately following the event published an epicentral estimate obtained from the analysis of seismic waves. As for the hypocentral depth, a good estimate was derived by *Oddone* [1909] from the intensity distribution, using the relation between source depth and intensity attenuation published by *Von Kovesligethy* [1906]; 9 km for the hypocentral depth and  $0.02 \text{ km}^{-1}$  for the intensity attenuation factor.

## 2.2. Tsunami observations

In addition to the earthquake felt reports, *Baratta* [1910] also listed a number of observations on the height of the tsunami wave from eyewitness accounts. *Platania* [1909] focused on these accounts, making geodetic measurements of the level reached by the tsunami waves and estimating their period and direction of approach. Overall, including the studies of both *Platania* [1909] and *Baratta* [1910], more than 130 localities were surveyed. The mean run-up height, measured along a 300 km-long segment of the eastern Sicily coast, was about 5 m, while the strongest effects occurred on a 80 km-long stretch from Galati Marina to Aci Trezza, with waves between 5 and 12 m in height (**Figure 2**). In the same paper *Platania* [1909] reported mareograms from different stations (**Figure 3**). The tsunami was recorded by the mareograph of Malta (about 250 km south of the epicenter) where the waves arrived about one hour after the earthquake and reached peak-to-peak amplitude as large as 90 cm with a period of about 20 minutes. North of the Messina Straits,

the tsunami was recorded by the mareographs located in the harbors of Naples, Ischia and Civitavecchia. The mareograph of Palermo was not functioning at the time of the earthquake. Back in operation around noon of the same day, it immediately started recording sea levels oscillations slightly smaller than 20 cm with a period of about 10 minutes. *Platania* [1909] attempted a physical interpretation of the tsunami wave velocity in connection with changes of sea floor depth. The basic theory of sea wave propagation and the gross bathymetry of the Straits area were already known, but the lack of computational facilities and the poor knowledge of the earthquake source physics did not allow any further analysis of the tsunami.

### **2.3. Instrumental observations: geodetic**

*Antonio Loperfido* [1909], an officer with the Italian Istituto Geografico Militare, remeasured two leveling lines fortuitously surveyed shortly before the earthquake, obtaining elevation changes at 114 benchmarks. Most of them (82) were located on the Calabrian shore and only a few (32) were on the Sicilian side of the Straits, between Messina and the crest of the Monti Peloritani (**Figure 4**). The density of the benchmarks and the accuracy of the measuring procedures were comparable to present day, but a fraction of the benchmarks subsided as a consequence of local settling of loose deposits, as remarked by *Loperfido* [1909] himself and by *De Stefani* [1909b]. Nevertheless the pattern of elevation changes appeared rather smooth and internally coherent, as expected for the surface signature of slip on a large normal fault, peaking at 54 cm in Reggio Calabria and nearly 70 cm in Messina.



## 2.4. Instrumental observations: seismological

Shortly after the earthquake many investigators published analyses based on a few or even on individual seismograms (e.g., *Agamennone* [1909]; *Comas Sola* [1909]; *Galitzin* [1909]; *Malladra* [1909]; see **Figure 5**). The analyses described particular aspects of the recordings but were generally not focused on the study of the earthquake source. The analysis of the first pulse at close stations carried out by *Omori* [1909] was one of the few attempts to get insight into the source characteristics. He concluded that the direction of the first displacement excluded a volcanic explosion as a possible cause of the earthquake.

The most complete compilation of seismological instrumental information was published by *Rizzo* [1910], who retrieved data from his fellow seismologists from all over the world. In addition to the reproduction of several original seismograms, *Rizzo* [1910] published parametric data for many stations that had recorded the earthquake, including their exact geographic coordinates, the earthquake arrival time and the amplitude of the different phases. He indicated 04:20:27 as the arrival time of the first pulse at the Messina station and assumed this as the origin time of the earthquake, but no associated error was indicated. Overall *Rizzo* listed 110 stations at regional and teleseismic distance. Unfortunately, not too much could be done at the time with this rich crop of data except for estimates of the origin time and of an unreliably large hypocentral depth.

## 3. New analyses: the instrumental era

Significant advances in Earth sciences were achieved during the decades immediately following the 1908 earthquake. Many seismologists published studies on the structure of the Earth's interior from the analysis of seismic data (e.g., *Mohorovičić* [1910]; *Gutenberg* [1912]; *Jeffreys* [1926] *Lehmann* [1936]) and the physical measure of the strength of radiated seismic waves (e.g., *Richter* [1935]; *Gutenberg* [1945a, 1945b]).

The early 1960's marked the beginning of a period of great progress for the Earth sciences and for seismology in particular. The deployment of worldwide instrumental networks gave a great boost to the development of seismological theory, modeling, and data analysis. New concepts for describing the seismic source, such as the seismic moment, double-couple, and fault plane solution, were quickly becoming part of the routine earthquake analysis.

Many past earthquakes were reconsidered in the light of the newly acquired knowledge. Being the largest earthquake ever recorded in Europe, and one the strongest worldwide, the 1908 event was of particular interest for seismologists. Moreover, at the beginning of the 1970s the Italian government decided to launch a project for a bridge crossing the Messina Straits that would permanently bind Sicily to the mainland. The technical solution that was later selected for this task is a 3 km-long, single span bridge. Although the project is still at a rather initial stage, building the longest single-span bridge in the world in a highly active area such as the Messina Straits requires accurate control and confident knowledge of the design earthquake, starting a new era of monitoring and analysis of the region's seismicity. At the beginning of a new phase of investigations of the 1908 earthquake prompted by the new engineering project, the intensity pattern and a rough location of the event were its sole known source characteristics. The intensity reports were reanalyzed with updated evaluation and field drawing criteria (e.g., *Bottari et al.* [1986]), but

the crucial contributions to the understanding of this earthquake came from the processing of the large crop of instrumental data (**Table 1**).

### 3.1. Seismographic data

The first modern studies based on the instrumental data concerned the evaluation of the magnitude of the 1908 earthquake. *Gutenberg and Richter* [1954] included 1908 in their catalog of global seismicity, assigning it a magnitude  $M_L=7\frac{1}{2}$ , the largest magnitude ever assigned to this event. As reported in **Table 2**, several other investigators determined its magnitude, sometimes from single or a few seismograms, using different magnitude scales ( $M_L$ ,  $m_B$ ,  $M_S$ ,  $M_W$ ). These investigators generally obtained similar values, mostly between 6.9 and 7.2. By allowing a direct comparison with other great earthquakes, this objective measure of the earthquake strength made it clear that its severity went beyond what was expected based on its magnitude. This evidence was consistent with, and somehow confirmed, *Mercalli's* [1909] and *Omori's* [1909] intuition about the role of poor building construction practice in increasing the effects of the earthquake.

A thorough analysis of the available instrumental data was accomplished by *Schick* [1977]. Based on *P* wave arrival times at a couple of close stations, he located the initiation of the rupture in the middle of the Messina Straits, a few kilometers south of the “seismic centers“ indicated by *Omori* [1910] and *Baratta* [1910], and concluded that from there the rupture had propagated to the north. Extending the initial work of *Riuscetti and Schick* [1974], he also evaluated the body wave and surface wave magnitudes on original seismograms from amplitude data of at least 10 stations

given by *Rizzo* [1910]. Except for 3 stations in Japan, his results were quite stable, mostly ranging between 6.9 and 7.1, giving on average  $m_B=7.0$  and  $M_S=7.1$ .

*Riuscetti and Schick* [1974] and *Schick* [1977] also attempted an assessment of  $M_0$ . The concept of seismic moment had been introduced shortly before [*Aki*, 1966], but at that time the relatively poor knowledge of the Earth structure and the limited modeling and analysis tools did not allow it to be determined with confidence. By making several assumptions these two studies determined  $M_0$  from body or surface waves. The authors used a single seismogram in both cases, obtaining  $5 \times 10^{18}$  and  $5 \times 10^{17}$  N m for body and surface waves, respectively. These figures were significantly different from each other and overall just too small when compared to the magnitude estimates. According to *Schick* [1977], this discrepancy was to be ascribed to a much lower crustal rigidity  $\mu$  than expected in the source area.

Using polarities of 11 first arrivals, *Riuscetti and Schick* [1974] derived the first fault plane solution for the 1908 event. Their nodal planes were oriented roughly parallel to the Sicilian coast (N20°E) and dipped 70° toward the WNW and 20° toward the ESE, accommodating approximately E-W extension. “*There is not much doubt that the Messina earthquake was accompanied by normal faulting*” was their conclusion. This result was then confirmed by all successive studies, even those with an increased number of polarities, with the sole variations of a small component of lateral slip and changes (minor but tectonically significant) in the strike of the nodal planes (see **Figure 6** and **Table 2**). The only significant exception to the interpretation of 1908 being a normal faulting earthquake was that of *Brogan et al.* [1975], who envisioned a possible origin of the 1908 earthquake as a compressional event that originated in the frame of the subduction of the Calabrian Arc. We remark that, up to this point, all investigation based on the instrumental seismological

record concerned only first arrivals (arrival time and polarity) and P-wave amplitudes for magnitude evaluation; no analysis of the complete waveforms was attempted.

### 3.2. Geodetic data

The application of the dislocation theory to the study of the earthquake source significantly increased during the late 1950's-early 1960's, making the modeling of geodetic data a viable method for gaining information on faulting processes (e.g., *Maruyama* [1964]). A full exploitation of leveling data, however, could be achieved only when modern computing tools became widely available. Almost 70 years after the Messina Straits earthquake, its source was investigated using the elevation changes meticulously collected by *Loperfido* [1909]. Again, *Schick* [1977] pioneered the application of the new ideas to the 1908 event, even though his geodetic analysis was limited to a qualitative comparison of the data with a number of curves computed for generic 45°-dipping normal faults. The original leveling data showed significant subsidence on both sides of the Messina Straits and mild uplift of the adjacent ranges. This pattern was incompatible with any of the used theoretical curves, particularly for a source located in the middle of the Straits. This inconsistency drove *Schick* [1977] to the conclusion that the earthquake was generated by a unilateral sinking force superposed on a single couple dislocation, with the latter corresponding to the west dipping plane of the focal mechanism of *Riuscetti and Schick* [1974] and *Schick* [1977] (**Figure 6**; model A in **Figure 7**). Based on a similar qualitative approach, *Caputo* [1980] proposed a mechanism with a similar strike and a 50°-60° west-dipping plane.

*Mulargia and Boschi* [1983] made a significant progress in analyzing the geodetic data by computing the displacement field of model faults for the specific earthquake. They searched for the best fitting focal mechanism and fault parameters by matching the theoretical and real elevation changes in a trial-and-error scheme. The characteristics of the method required the separate modeling of 3 distinct subsets of the leveling data and the assumption of constant slip on the fault. The data were fit reasonably well by a 1.5 m dislocation of a graben-like structure formed by two parallel and quasi-antithetic faults: an east-dipping, low-angle fault located near the northern end of the Straits, and a smaller, west-dipping, subvertical fault located more to the south, on the Calabrian side of the Straits (**Figures 6, 7** model B). The nodal planes of their focal mechanism were very similar to those proposed by *Riuscetti and Schick* [1974] and *Schick* [1977].

With the fast increment in the computing skills and the larger availability of computers, the solution of the inverse problem became reality, and the elevation changes collected by *Loperfido* [1909] demonstrated all their potential. *Capuano et al.* [1988] first applied an inversion algorithm to these data searching for the best fitting dislocation model. Their model fault consisted of several uniform slip rectangular segments compatible with a focal mechanism derived from 23 first motion polarities. Unlike the fault plane solution proposed by *Riuscetti and Schick* [1974], their mechanism (**Figure 6**) displayed a significant lateral component which, coupled with the results of the analysis of elevation changes, resulted in a  $\sim 25^\circ$  difference in the strike of the fault, oriented N10W°. Though not large, this discrepancy is tectonically significant in the context of the Messina Straits. The results of *Capuano et al.* [1988] are characterized by a larger dislocation patch in the southern portion of the rupture and by a 56.7 km-long fault with the northern end well beyond the end of the Messina Straits proper (D in **Figure 7**). They remarked that the fit of four benchmarks located in the Messina harbor forced the fault to shift westward by as much as 10 km. The reliability of these

benchmarks, displaying significant subsidence (up to about 70 cm) in a very limited area, has been debated since the time of the earthquake. *Loperfido* [1909], as well as *De Stefani* [1909b], contended that local collapse phenomena occurred along the line.

Giving credit to these considerations, *Boschi et al.* [1989] discarded the Messina harbor benchmarks and analyzed a dataset dominated by observations from the Calabrian side of the Straits. They also contended that the Messina harbor benchmarks would have a very limited resolving power and would essentially be blind to slip on the deeper portion of the fault. They inverted the geodetic data for the focal mechanism first by imposing uniform dislocation and found that the data are well satisfied by a low angle, east dipping fault very similar to that proposed by *Schick* [1977] and to the northern fault of *Mulargia and Boschi* [1983] (**Figure 6**; model E in **Figure 7**); then derived a slip distribution characterized by two main slip patches, with the largest displacement of about 3 m nearly coincident with larger slip patch of *Capuano et al.* [1988].

Shortly after *De Natale and Pingue* [1991] presented the results of a further inversion for variable slip. Their solution was based on the model fault proposed by *Capuano et al.* [1988] and included all the controversial Messina harbor benchmarks (model F in **Figure 7**). Apart from the fault strike, the main difference between their solution and that presented by *Boschi et al.* [1989] was the obvious presence of a pronounced slip maximum beneath the Messina harbor. The results obtained for the seismic moment by these different groups were very consistent, stressing the robustness of models based on elevation changes:  $6.2 \times 10^{19}$  N m for *Capuano et al.* [1988];  $3.7 \times 10^{19}$  N m for *Boschi et al.* [1989];  $3.5 \times 10^{19}$  N m for *De Natale and Pingue* [1991].

The proposed models still showed some scatter, for example concerning the exact orientation of the fault and its length, partly originating from the data themselves (e.g., unreliability of the Messina benchmarks) and partly from modeling options. Nevertheless, the picture was slowly

coming into focus, and the variability between different solutions (see **Table 2** and models B, D, E, F in **Figure 7**) turned out to be only slightly larger than that expected for much more recent large earthquakes.

### **3.3. Early analyses of the tsunami**

The investigations of the tsunami that followed the 1908 earthquake hold an important place in the long list of the papers that reconsidered this earthquake in the light of modern methods of analysis. The introduction of scales for measuring the magnitude of a tsunami and its relation with the associated earthquake (e.g., *Iida* [1963]; *Kajiura* [1981]) favored the comparison of the 1908 Messina Straits event with other known tsunamigenic earthquakes. *Caputo* [1980] and *Tinti and Giuliani* [1983] were the first to review the instrumental recordings and the maximum run-up data reported by *Platania* [1909]. Both these studies critically analyzed the high ratio between the maximum wave height and the earthquake magnitude, stressing the role of the bathymetry of the Messina Straits in generating unusually high sea waves.

All in all, the approach taken by these workers was still rather simplistic, as sophisticated tsunami models required a detailed knowledge of the bathymetry of the region under investigation (e.g., with a spatial resolution of 100 m or better) and significant computational facilities: unfortunately, both these conditions were definitely at a premature stage at the beginning of the 1980s.



#### 4. The recent reappraisal: exploiting the technical development

The 1990s marked great scientific and technological progresses in seismology worldwide. The evolution of instrumentation was rapidly followed by the development of improved data processing techniques. New findings on the structure of the inner Earth and the seismic source produced new ideas and opened new fields of investigation. Studies of the links between crustal tectonics and faulting, of the interaction between tectonic stress and preexisting faults, on the relations between small and large magnitude events became crucial topics in earthquake science. During the same decade the public concern about natural hazards greatly increased, and the demand for risk mitigation pushed the scientific community to address focused studies. The investigation of old earthquakes became crucial in a country like Italy, where thousands of small earthquakes are recorded yearly but slip rates are relatively low and large earthquakes occur every 1,000-3,000 years [Basili *et al.*, 2008; Galli *et al.*, 2008]; a fortunate condition but also one that makes the identification of major earthquake sources especially difficult. The study of the main seismogenic sources may certainly benefit from the analysis of instrumental earthquakes with modern techniques (e.g., joint or double-differences location), but the full understanding of their geometry and recurrence characteristics relies on the investigation of past large earthquakes such as 1908.

The scientific - but also social and political - interest for the 1908 earthquake was further increased by the apparently imminent construction of the bridge across the Straits. After several decades of relatively slow progress and elaboration, powerful computers and new tools analysis of and processing - for example optical scanning and digitizing of old seismograms - were now making it possible to deal with historical instrumental data using modern techniques (**Table 1**). Meanwhile, forward and inverse modeling of seismometric, geodetic, and mareometric data also

greatly developed and became routine since the mid 1990s. Studies such that of *Piatanesi et al.* [1999] would have been much more difficult and time-consuming just a few years back for standard computing facilities. These investigators performed a finite-elements simulation of the 1908 tsunami, and used a mesh consisting of more than 16,000 elements, to compute synthetic mareograms for two different source mechanisms, those of *Capuano et al.* [1988] and *Boschi et al.* [1989] (models D and E in **Figure 7**, respectively). However, due to computational limitations, their analysis was limited to a comparison of the polarity of the first impacting wave and the pattern of the run-up heights. *Piatanesi et al.* [1999] concluded that, in comparison with the *Capuano et al.* [1988] model, the source proposed by *Boschi et al.* [1989] gives a better – but still rather poor - fit to the data.

*Tinti et al.* [1999] tried to improve the match between observed run-up values and computed maximum tsunami levels by allowing heterogeneous slip on the fault. Their conclusion was that a better agreement resulted with most slip being released in the southern part of the fault. However, it is worth noting that all the seismic sources tested by *Piatanesi et al.* [1999] and *Tinti et al.* [1999] are unable to explain the overall observed height of the tsunami; both of these papers underestimated the maximum wave heights by a factor of 4-5 with respect to the actual run-ups, leaving the determination of the tsunamigenic source an unsolved problem.

*Pino et al.* [2000] analyzed the digitized waveforms of the original historical seismograms. This has been a relatively simple task following the inception of *SISMOS* [*Michelini et al.*, 2005a] and *Euroseismos* [*Ferrari and Pino*, 2003], two projects aimed at collecting and digitizing historical seismograms and at developing new strategies for their analysis. By inverting *P* waveforms, *Pino et al.* [2000] derived source time functions and obtained an estimate of the seismic moment of  $5.38 \times 10^{19}$  N m, corresponding to a moment magnitude  $M_w=7.1$  (**Figure 8a**). From direct modeling

of *SH* waveforms (**Figure 8b**) they also inferred that the earthquake was generated by unilateral rupture with northward directivity over a 43 km-long fault, and turned the derived source time function into a slip distribution assuming an average rupture velocity of 2 km/s. Overall, their conclusions were in good agreement with previous geodetic results, with the only exception that they found no evidence for the significant dislocation beneath the Messina harbor reported by *De Natale and Pingue* [1991], pointing to a limited reliability of the Messina harbor benchmarks (**Figure 9**). The correspondence between the slip distribution independently derived from seismological and geodetic data was considered by *Pino et al.* [2000] as a definite support for the assumed rupture velocity. Unfortunately, all analyzed seismograms were written by stations located in northern Europe; the large azimuthal gap made it impossible to discriminate unambiguously between the focal mechanisms of *Capuano et al.* [1988] and *Boschi et al.* [1989] based on waveform modeling alone.

*Amoruso et al.* [2002] performed a joint inversion of the geodetic data and of the *P*-wave first motion polarities. Their results for the focal mechanism were very similar to those of *Capuano et al.* [1988] and *De Natale and Pingue* [1991], but they obtained significant dislocation over a nearly 100 km-long fault (**Figure 9**). Their model fault extends beyond the northern end of the Straits and south of the previously estimated epicenter; both areas that are poorly illuminated by the available elevation changes (model G in **Figure 7**).

Finally, *Michelini et al.* [2005b] attempted a relocation of the earthquake epicenter based on *NonLinLoc* (NLL) [*Lomax*, 2005], a code performing a probabilistic location using an importance-sampling method based on an efficient global cascading grid-search. The result is independent of the origin time estimate and insensitive to the presence of outliers. These features make NLL particularly suitable for the location of historical earthquakes. The epicenter of *Michelini et al.*

[2005b] substantially confirmed the previous locations and, combined with the unilateral nature of the rupture, ruled out the possibility of significant dislocation south of the epicenter.

## **5. Discussion: a century of investigations**

During the past 100 years, tens of scientists have contributed to develop a complete description of the 1908 Messina Straits earthquake as if it were a much more recent event. This was made possible by the progressive advancement in the understanding of the seismic source, but also by the invaluable sets of data collected by the pioneers of seismology at the time of the earthquake. **Table 1** summarizes the main milestones in the progress of the investigations.

### **5.1. Summary of the source model**

The combination of the conclusions from the geodetic and seismological analyses, along with hints from the regional tectonic setting, constrains well the geometry and extent of the fault and its rupture style. The 1908 earthquake was caused by dominantly normal slip on an approximately NNE-SSW trending plane dipping to the east, extending from about 3 to 12 km depth and for a length of 40-45 km from the epicenter in the south to the northern end of the Straits.

The rupture initiated at  $37.96^{\circ}$  N,  $15.71^{\circ}$  E and propagated unilaterally northward at about 2 km/s. The slip pattern exhibits three main patches of dislocation, with a maximum of 3-4 m slightly south of the city of Reggio Calabria and an average of 1.5-2.0 m. The seismic moment associated

with the event is bracketed by the estimates obtained from geodetic ( $3.5 \times 10^{19}$  N m) and seismological data ( $5.4 \times 10^{19}$  N m), corresponding to a moment magnitude in the range  $M_W=7.0-7.1$ .

Both the geodetic and seismological estimates of the rupture length carry uncertainties, but fortunately they tend to compensate. Due to the geometry of the leveling network in relation to the earthquake source, the inversions of the elevation changes are most sensitive to the central portion of the fault at depth but leave the mid and shallow portion of the fault largely unresolved. Similarly, the actual location of the southern end of the fault is poorly resolved by the leveling network. This may have led to a significant underestimation of coseismic slip, and therefore of the seismic moment. The seismological estimates of the rupture length, however, suggest that the rupture did not exceed 40-45 km (**Figure 9**) and that the earthquake causative fault lies entirely within the Messina Straits proper. Thus, the seismic moment/magnitude range is asymmetric and higher values are to be preferred, but the upper bound of the range appears to be rather tightly constrained.

The exact strike of the fault plane from geodetic evidence is still uncertain, depending on whether or not the Messina harbor benchmarks are included in the computations. The results of the seismic waveform analysis, however, combined with geologic and tectonic evidence suggest that the Messina benchmarks recorded a combination of tectonic and non-tectonic subsidence, and that a NNE-striking fault plane satisfies better all available evidence.

The resulting source model is very similar to that proposed by *Boschi et al.* [1989] (E in **Figure 7**). **Figure 10** shows the match between the fault location, size and orientation and the rupture directivity on the one hand, and the damage pattern on the other hand. Aside from site effects, this source model explains well the differential decay of intensity on the two shores of Straits and the much larger damage suffered by Calabrian cities and villages (see also **Figure 1b**).

## 5.2. Open issues: understanding the source of the tsunami

The image of the 1908 earthquake stemming from a century of investigations is rather coherent and only a few significant uncertainties still remain. Perhaps the only really open issue concerns the causative source of the strong tsunami. Very recently, two papers reached substantially opposite conclusions and further stirred the debate on this issue. *Billi et al.* [2008] proposed that the origin of the tsunami must be related to a large submarine landslide, set in motion by the strong shaking and/or the stress transfer induced by the earthquake; conversely, *Gerardi et al.* [2008] contended that the pattern of run-ups along the Calabrian and Sicilian coasts is more compatible with a tsunami generated by tectonic dislocation of the sea floor than with a tsunami resulting from a submarine landslide. Solving this problem requires even more accurate tsunami calculations than those already performed by *Piatanesi et al.* [1999] and *Tinti et al.* [1999], including the modeling of the inundation phase using very detailed bathymetry and topography. It has been shown that the inversion of tide gauge records allows for the determination of some important characteristics of the rupture process, for example the slip distribution on the fault plane [e.g. *Satake*, 1987; *Hirata et al.*, 2003; *Piatanesi and Lorito*, 2007; *Lorito et al.*, 2008a]; this technique has been successfully applied also to historical events such as the 1906 San Francisco earthquake [*Lorito et al.*, 2008b]. For the 1908 Messina tsunami there exist tide gauge records for Malta, Napoli, Ischia, Civitavecchia and Palermo (**Figure 3**). These have not yet been used in a quantitative fashion, but could offer new important constraints to determine the characteristics of the tsunamigenic source.

### 5.3. The 1908 earthquake: geodynamic framework and recurrence characteristics

The Messina Straits cuts with a NNE-SSW trend the southern Calabrian Arc. This large geodynamic feature comprises the surface evidence of the northwestward subduction of the Ionian lithosphere, separating the African plate from the thinned back arc Tyrrhenian basin. During the Pliocene and Pleistocene, the Calabrian Arc has experienced rapid uplift along a trend parallel to the arc axis, leading to the activation of arc-parallel half-graben structures [Ghisetti, 1984; Westaway, 1993; Bordonì and Valensise, 1998; DISS Working Group, 2007; Basili *et al.*, 2008]. The longitudinal fault system is segmented by transversal NW-SE and E-W structures, also detectable in the peri-Tyrrhenian basins [Fabbri *et al.*, 1980; Barone *et al.*, 1982]. The Straits itself is one of these N-S half-Grabens [Ghisetti, 1992], bent in the E-W direction at its northern end [Selli *et al.*, 1978]. Reliable GPS measurements suggest large strains (~100 nanostrain/y) and extension perpendicular to the axis of the Messina Straits at a rate ranging from 3.6 mm/y [D'Agostino and Selvaggi, 2004] to 2.0 mm/y [Serpelloni *et al.*, 2007], in agreement with the E-W to ESE WNW extension shown by the focal mechanisms obtained for the 1908 earthquake.

Multiple lines of evidence thus suggest that the causative fault of the 1908 earthquake plays a major role in the geodynamic evolution of the Calabrian Arc. By comparing the 1908 coseismic elevation changes with topographic and geomorphic features, Valensise and Pantosti [1992] proposed that repeated 1908-type earthquakes, with similar dislocation along similar fault length, have largely shaped up the present structure of the Messina Straits (**Figure 11**). Moreover, by comparing the coseismic elevation changes and the elevation of a well dated geological marker they estimated a repeat time of 1908-type earthquakes of 1,000 years (+500, -300) and an average extension rate of 1.2 mm/y across the Messina Straits, corresponding to a minimum fault slip rate of

1.4 mm/y. The seismological evidence for a larger seismic moment than that determined geodetically suggests that actual repeat times are close to the upper limit of the above interval, as also indicated by historical and archeological evidence [*Guidoboni et al.* 2000]. According to *D'Agostino and Selvaggi* [2004], however, up to 80% of the 3.6 mm/yr relative motion between the Sicilian and Calabrian blocks may be accommodated in the Messina Straits, loading the fault responsible for the 1908 earthquake. This would imply somewhat faster extension and correspondingly shorter recurrence intervals. But, if both the geological and geodetic estimates are accurate, either significant deformation occurs aseismically, or else other – presumably secondary - faults are required to accommodate this relative motion. Conversely, the 2.0 mm/y extension rate estimated by *Serpelloni et al.* [2007] requires no extra strain to be accommodated across the Straits in addition to that associated with 1908-type earthquakes.

Whatever the case, the fault responsible for the 1908, 28 December, Messina Straits catastrophic earthquake is definitely a major seismogenic structure capable of  $M_w=7.1$  events lying beneath a densely populated area. The image developed throughout a century of investigations represents fundamental knowledge for the prediction of the ground motion in case of repetition of a strong earthquake, and becomes of special value in the design of major infrastructures, such as the planned permanent crossing of the Straits.



## References

- Agamennone, G. (1909), Importante particolarità nei sismogrammi del Regio Osservatorio Geodinamico di Rocca di Papa in occasione dei terremoti calabro-siciliani dell'8 settembre 1905 e 28 dicembre 1908, *Atti Regia Acc. Lincei. Rendiconti*, 18, 339-343.
- Aki, K. (1966), Generation and propagation of G waves from the Niigata earthquake of June 16, 1964: Part 2. Estimation of earthquake moment, released energy, and stress-strain drop from the G wave spectrum, *Bull. Earthquake Res. Inst. Tokyo Univ.*, 44, 73-88.
- Amoruso A., L. Crescentini, and R. Scarpa (2002), Source parameters of the 1908 Messina Straits, Italy, earthquake from geodetic and seismic data, *J. Geophys. Res.*, 107 (B4), 2080, doi:10.1029/2001JB000434.
- Baratta, M. (1910), La catastrofe sismica calabro-messinese 28 dicembre 1908, relazione, Soc. Geogr. It., Rome.
- Barone, A., A. Fabbri, S. Rossi, and R. Sartori (1982), Geological structure and evolution of the marine areas adjacent to the Calabrian Arc, in *Structure, evolution and present dynamics of the Calabrian Arc*, edited by E. Mantovani and R. Sartori, *Earth Evol. Sci.*, 3, 207-221.
- Basili, R., G. Valensise, P. Vannoli, P. Burrato, U. Fracassi, S. Mariano, M. Tiberti and E. Boschi (2008), The Database of Individual Seismogenic Sources (DISS), version 3: summarizing 20 years of research on Italy's earthquake geology, *Tectonophysics*, 453, 20-43, doi:10.1016/j.tecto.2007.04.014.
- Billi A., R. Funiciello, L. Minelli, C. Faccenna, G. Neri, B. Orecchio, D. Presti (2008), On the cause of the 1908 Messina tsunami, southern Italy, *Geophys. Res. Lett.*, 35, L06301, doi:10.1029/2008GL033251.
- Bordoni, P. and G. Valensise (1998), Deformation of the 125 ka marine terrace in Italy: tectonic implications. In: Stewart I. S. and Vita Finzi C. (eds), *Late Quaternary coastal tectonics*, Geological Society, London, Special Publications, 146, 71-110.
- Boschi, E., G. Ferrari, P. Gasperini, E. Guidoboni, G. Smriglio and G. Valensise (1995). Catalogo dei forti terremoti in Italia dal 461 a.C. al 1980, ING-SGA, Bologna, 973 pp. and a CD-ROM.
- Boschi, E., D. Pantosti, and G. Valensise (1989), Modello di sorgente per il terremoto di Messina del 1908 ed evoluzione recente dell'area dello Stretto, *Atti VIII Convegno G.N.G.T.S., Roma*, 245-258.
- Bottari, A., E. Carapezza, M. Carapezza, P. Carveni, F. Cefali, E. Lo Giudice, and C. Pandolfo (1986), The 1908 Messina Strait earthquake in the regional geostructural framework, *Journal of Geodynamics*, 5, 275-302.
- Brogan, G. E., L.S. Cluff and C. L. Taylor (1975), Seismicity and uplift of southern Italy, *Tectonophysics*, 29, 323-330.
- Capuano, P., G. De Natale, P. Gasparini, F. Pingue, and R. Scarpa (1988), A model for the 1908 Messina Straits (Italy) earthquake by inversion of leveling data, *Bull. Seismol. Soc. Am.*, 78, 1930-1947.
- Caputo, M. (1980), Seismicity in the Straits of Messina, *Atti Convegno Stretto di Messina, Accad. Naz. Lincei*, 101-117.
- Comas Sola, J. (1909), Le tremblement de terre du 28 d'Écembre 1908, enregist. l'Observatoire Fabra (Barcelone), *Comp. Ren. Séances Acad. Sci.*, 148, 202-203.
- D'Agostino, N., and G. Selvaggi (2004), Crustal motion along the Eurasia-Nubia plate boundary in the Calabrian Arc and Sicily and active extension in the Messina Straits from GPS measurements, *J. Geophys. Res.*, 109, B11402, doi:10.1029/2004JB002998.
- De Natale, G., and F. Pingue (1991), A variable slip fault model for the 1908 Messina Straits (Italy) earthquake, by inversion of leveling data, *Geophys. J. Int.*, 104, 73-84, 1991.
- De Stefani, C. (1909a), Riassunto delle osservazioni fatte dopo il terremoto calabro-siculo del 1908, Relazione della Commissione Reale incaricata di designare le zone più adatte per la ricostruzione degli abitati colpiti dal terremoto del 28 dicembre 1908 o da altri precedenti, 97-105.
- De Stefani, C. (1909b), La livellazione sul litorale calabro-siculo dopo il terremoto del 1908, *Boll. Soc. Geol. It.*, 29.
- Dewey, J., and P. Byerly (1969), The early history of seismometry (to 1900), *Bull. Seismol. Soc. Am.*, 59(1), 183-227.
- DISS Working Group (2007) – Database of Individual Seismogenic Sources (version 3.0.4): A compilation of potential sources for earthquakes larger than M 5.5 in Italy and surrounding areas. Available at: <http://www.ingv.it/DISS>.
- Fabbri, A., F. Ghesetti, and L. Vezzani (1980). The Peloritani-Calabria Range and the Gioia Basin in the Calabrian Arc (southern Italy): relationships between land and marine data. *Geologica Romana*, 19, 131-150.
- Ferrari, G., and N.A. Pino (2003), Euroseismos 2002-2003, a project for saving and studying historical seismograms in euro-mediterranean area, *Geophys. Abs.*, 5, 05274.
- Galitzin, B. (1909), Das sicilianische Erdbeben am 28 December 1908 nach den Aufzeichnungen der Pulkowa'schen seismischen Station, *Bull. Acad. Imp. Sci. St-Petersbourg*, 279-298.
- Galli P., F. Galadini and D. Pantosti (2008), Twenty years of paleoseismology in Italy, *Earth Science Review*, 88, 89-117.

- Gasparini, C., G. Iannaccone, P. Scandone, and R. Scarpa (1982), Seismotectonics of the Calabrian Arc, *Tectonophysics*, 84, 267-286.
- Gerardi, F., M. S. Barbano, P. M. De Martini and D. Pantosti (2008): Discrimination of tsunami sources (earthquake vs. landslide) on the basis of historical data in eastern Sicily and southern Calabria, *Bull. Seismol. Soc. Am.*, (in press).
- Ghisetti, F. (1984), Recent deformations and the seismogenic source in the Messina Strait (Southern Italy), *Tectonophysics*, 109, 191-208.
- Ghisetti, F. (1992), Fault parameters in the Messina Strait (Southern Italy) and relations with the seismogenic source, *Tectonophysics*, 210, 117-133.
- Gilbert, G. K. (1884), A theory of earthquakes of the Great Basin, with a practical application, *Amer. J. Sci.*, XXVII, 49-53.
- Guidoboni, E., A. Muggia, and G. Valensise (2000), Aims and methods in territorial archaeology: possible clues to a strong IV century A.D. earthquake in the Straits of Messina (southern Italy), in *The archaeology of geological catastrophes*, edited by B. McGuire, D. Griffiths, and I. Stewart, Geol. Soc., London, Spec. Publications, 171, 45-70.
- Guidoboni E., G. Ferrari, D. Mariotti, A. Comastri, G. Tarabusi and G. Valensise (2007), CFTI4Med, Catalogue of Strong Earthquakes in Italy (461 B.C.-1997) and Mediterranean Area (760 B.C.-1500). INGV-SGA. Available from <http://storing.ingv.it/cfti4med/>.
- Gutenberg, B. (1912), Ueber erdbebenwellen. VII A, Beobachtungen an registrierungen von fernbeben in Göttingen und folgerungen über die konstitution des erdkörpers, *Nachrichten von der Gesellschaft der Wissenschaften zu Göttingen, Mathematisch-Physikalische Klasse*, 125-176.
- Gutenberg, B. (1945a), Amplitudes of surface waves and magnitudes of shallow earthquakes, *Bull. Seismol. Soc. Am.*, 35, 3-12.
- Gutenberg, B. (1945b), Amplitudes of P, PP, and S and magnitudes of shallow earthquakes, *Bull. Seismol. Soc. Am.*, 35, 57-69.
- Gutenberg, B., and C.F. Richter (1954), Seismicity of the Earth and associated phenomena, 2nd ed., Princeton University Press, Princeton, N.J.
- Hirata, K., E. Geist, K. Satake, Y. Tanioka and S. Yamaki (2003), Slip distribution of the 1952 Tokachi-Oki earthquake ( $M$  8.1) along the Kuril Trench deduced from tsunami waveform inversion, *J. Geophys. Res.*, 108(B4), 2196, doi:10.1029/2002JB001976.
- Hoernes, R. (1878), Erdbeben studien, *Jahrb. Geol. Reichsanst.*, 28, 387-448.
- Iida, K. (1963), A relation of earthquake energy to tsunami energy and the estimation of the vertical displacement in a tsunami source, *J. Earth Sci.*, 2, 49-67.
- Jeffreys, H. (1926), The rigidity of the Earth's central core, *Monthly Notices R. Astron. Soc., Geophysical Supplement*, 1, 371-383.
- Kajiura, K. (1981), Tsunami energy in relation to parameters of earthquake fault model, *Bull. Earth. Res. Inst.*, 56, 415-440.
- Kárník, V. (1969), Seismicity of the European Area, Part 1, D. Reidel Publishing Company, Dordrecht, Holland.
- Lawson, A.C., chairman (1908), The California Earthquake of April 18, 1906: Report of the State Earthquake Investigation Commission, Carnegie Institution of Washington Publication 87, 1.
- Lehmann I. (1936), P', *Publications du Bureau Central Séismologique International*, A 14, 87-115.
- Lomax, A. (2005), A reanalysis of the hypocentral location and related observations for the great 1906 California earthquake, *Bull. Seismol. Soc. Am.*, 95(3), 861-877, doi:10.1785/0120040141.
- Loperfido, A. (1909), Livellazione geometrica di precisione eseguita dall'I.G.M. sulla costa orientale della Sicilia, da Messina a Catania, a Gesso ed a Faro Peloro e sulla costa occidentale della Calabria da Gioia Tauro a Melito di Porto Salvo, Relaz. Comm. Reale Acc. Naz. Lincei, Roma, 1909.
- Lorito, S., F. Romano, A. Piatanesi and E. Boschi (2008a): Source process of the September 12, 2007,  $M_w$  8.4 southern Sumatra earthquake from tsunami tide gauge record inversion, *Geophys. Res. Lett.*, 35, L02310, doi:10.1029/2007GL032661.
- Lorito, S., A. Piatanesi and A. Lomax (2008b): Rupture process of the April 18 1906 California earthquake from near-field tsunami waveform inversion, *Bull. Seismol. Soc. Am.*, 98(2), 832-845, doi:10.1785/0120060412.
- Malladra, A. (1909), Il sismogramma alpino del grande terremoto calabro-messinese, *Riv. Fis. Mat. Sci. Nat.*, 110, 5-32.
- Mallet, R. (1862). The great Neapolitan earthquake of 1857. The first principles of observational seismology, Chapman and Hill (Publ.), London.
- Martinelli, G. (1909), Osservazioni preliminari sul terremoto calabro-messinese del 28 dicembre 1908, *Boll. Bimens. Soc. Meteor., Ser. III*, 28.

- Maruyama, T. (1964), Statical elastic dislocation in an infinite and semi-infinite medium, *Bull. Earthquake Res. Inst. Tokyo Univ.*, 42, 289-368.
- Mercalli, G. (1909), Contributo allo studio del terremoto calabro-messinese del 28 dicembre 1908, *Atti Ist. Incoraggiamento Napoli*, 3, 1-46.
- Michelini, A., B. De Simoni, A. Amato, and E. Boschi (2005a), Collecting, digitizing, and distributing historical seismological data, *Eos Trans. AGU*, 86(28), 261, doi:10.1029/2005EO280002.
- Michelini, A., A. Lomax, A. Nardi, A. Rossi, B. Palombo, and A. Bono (2005b), A modern re-examination of the locations of the 1905 Calabria and the 1908 Messina Straits earthquakes, *Geophys. Res. Abs.*, 7, 07909.
- Mohorovičić, A. (1910), Das beben vom 8.10.1909, *Jarbuch des Meteorologischen Observatorium in Zagreb (Agram), für das Jahr 1909*, 9, 1-63.
- Mulargia, F., and E. Boschi (1983), The 1908 Messina earthquake and related seismicity, in *Earthquakes: observation, theory and interpretation*, edited by H. Kanamori and E. Boschi, Proc. Int. Sch. Phys. Enrico Fermi, Course LXXXV, 493-518.
- Oddone, E. (1909), Calcolo provvisorio della profondità dell'ipocentro del terremoto calabro-siculo del 28 dicembre 1908, *Atti Regia Acc. Lincei. Rendiconti*, 18, 186-192.
- Omori, E. (1909), Preliminary report on the Messina-Reggio earthquake of Dec. 28, 1908, *Bull. Imp. Earth. Comm.*, 3-2, 37-46.
- Perret, F.A. (1909), Preliminary report on the Messina earthquake of Decembre 28, 1908, *Am. Jour. of Science*, 27, 321-334.
- Piatanesi, A. and S. Lorito (2007) : Rupture process of the 2004 Sumatra-Andaman earthquake from tsunami waveform inversion, *Bull. Seismol. Soc. Am.*, 97(1), 223-231, doi :10.1785/0120050627.
- Piatanesi, A., S. Tinti, and E. Bortolucci (1999), Finite-elements simulations of the 28 December 1908 Messina Straits (southern Italy) tsunami, *Phys. Chem. Earth (A)*, 24, 145-150.
- Pino, N.A., D. Giardini, and E. Boschi (2000), The December 28, 1908, Messina Straits, southern Italy, earthquake: Waveform modeling of regional seismograms, *J. Geophys. Res.*, 105(B11), 25,473-25,492.
- Platania, G. (1909), Il maremoto dello Stretto di Messina del 28 dicembre 1908, *Boll. Soc. Sismol. It.*, 13, 369-458.
- Reid, H.F. (1910), The mechanics of the earthquake, in *The California Earthquake of April 18, 1906: Report of the State Earthquake Investigation Commission*, Carnegie Institution of Washington Publication 87, 2.
- Richter, C. F. (1935). An instrumental earthquake magnitude scale, *Bull. Seismol. Soc. Am.*, 25, 1-32.
- Ritter, J.R.R. (2002), On the recording characteristics of the original Wiechert seismographs at Göttingen (Germany), *J. of Seimol.*, 6, 477-486.
- Riuscetti, M., and R. Schick R. (1974), Earthquakes and tectonics in Southern Italy, *Proc. Joint Symp. Eur. Seismol. Comm. and Eur. Geophys. Soc.*, 59-78.
- Rizzo, G.B. (1910), Sulla propagazione dei movimenti prodotti dal terremoto di Messina del 28 dicembre 1908, *Mem. R. Accad. Sci. Torino, Ser. II*, 61.
- Satake, K. (1987). Inversion of tsunami waveforms for the estimation of a fault heterogeneity: method and numerical experiments, *J. Phys. Earth*, 35, 241-254.
- Schick, R. (1977), Eine seismotektonische Bearbeitung des Erdbebens von Messina im Jahre 1908, *Geol. Jahrb.*, 11, 3-74.
- Selli, R., P. Colantoni, A. Fabbri, S. Rossi, A.M. Borsetti, and P. Gallignani (1978), Marine geological investigation of the Messina Strait and its approaches, *Giornale di Geologia*, 42, 1-70.
- Serpelloni, E., G. Vannucci, S. Pondrelli, A. Argnani, G. Casula, M. Anzidei, P. Baldi, and P. Gasperini (2007), Kinematics of the Western Africa-Eurasia plate boundary from focal mechanisms and GPS data, *Geophys. J. Int.*, doi: 10.1111/j.1365-246X.2007.03367.2007.
- Tinti, S., A. Armigliato, E. Bortolucci, and A. Piatanesi (1999), Identification of the source fault of the 1908 Messina earthquake through tsunami modelling. It is a possible task?, *Phis. Chem. Earth (B)*, 24, 417-421.
- Tinti, S., and D. Giuliani (1983), The Messina Straits tsunami of December 28, 1908: a critical review of experimental data and observations, *Il Nuovo cimento*, 6, 429-442.
- Valensise, G., and D. Pantosti (1992), A 125-Kyr-long geological record of seismic source repeatability: the Messina Straits (southern Italy) and the 1908 earthquake ( $M_S 7\frac{1}{2}$ ), *Terra Nova*, 4, 472-483.
- Von Kovesligethy, R. (1906), Seismonomia, *Boll. Soc. Sism. Ital.*, 14.
- Westaway, R. (1993), Quaternary uplift of Southern Italy, *J. Geophys. Res.*, 98, 21,741-21,772.

N. A. Pino,  
Istituto Nazionale di Geofisica e Vulcanologia,  
Osservatorio Vesuviano,  
Via Diocleziano 328, 80124, Naples, Italy.  
([napino@ov.ingv.it](mailto:napino@ov.ingv.it))

## Figure captions

**Figure 1.** a) Location map of the Messina Straits, showing selected historical earthquakes and the epicentral locations calculated by *Omori* [1909] and by *Baratta* [1910]. b) Intensity pattern of the 1908 earthquake (from *Baratta* [1910]). The dashed area suffered the strongest ground shaking. Notice the different decay of intensity on either side of the Straits and the strong asymmetry of damage toward Calabria.

**Figure 2.** a) Overview of coastal sites for which a measure of run-up is available (*Gerardi et al.*, 2008). Red dots indicate coastal sites along the Sicilian coast, negative numbers indicate the distance of the sites from the origin point (Punta Faro). Yellow triangles mark coastal sites along the Calabrian coast, positive numbers indicate the distance of the sites from the origin point (Porto S. Venera). b) Red dots and yellow triangles represent the measured run-up heights along the Sicilian and Calabrian coasts, respectively.

**Figure 3.** a) Location of tide-gauge stations that recorded the tsunami (yellow dots). The red transparent ellipse indicates the source area of the earthquake. b) Original tide-gauge records of the tsunami, as reported in *Platania* [1909]. From top to bottom: Palermo, Napoli, Civitavecchia, Ischia and Malta. Note that time runs from right to left in the record of Malta.

**Figure 4.** Overview of the elevation changes measured by *Loperfido* [1909] following the 1908 earthquake (in cm). The largest tectonic subsidence was recorded in Reggio Calabria. The Messina harbour also experienced subsidence up to 70 cm, but the observed values are suspected to reflect at least partially non-tectonic deformation due to settling of coastal deposits.

**Figure 5.** (left) Example of an original seismogram written by the 1908 earthquake on the 1200 kg Wiechert instrument at Plauen (Germany), and (right) the corresponding digitized and corrected waveform. The original seismogram shows clearly the effects of the finite length and inclination of the arm.

**Figure 6.** Summary of available fault plane solutions for the 1908 earthquake. If indicated, the preferred fault plane is shown by a blue arrow.

**Figure 7.** Surface projection of the published fault planes for the 1908 earthquake. A red line marks the intersection of the fault plane with the surface (cut-off line), and hence shows the direction of dip of the fault (but notice that all faults are explicitly or implicitly assumed to be blind).

**Figure 8.** a) On the right are illustrated the recorded data (continuous line) for the 1908 earthquake and synthetic *P* wave seismograms obtained by *Pino et al.* [2000] for different German stations (PLN, Plauen; LEI, Lipsia; GTT, Göttingen; POT, Potsdam; the small letter indicates the component). Synthetics result from waveform inversion performed for two different structural models. The numbers indicate the resulting seismic moment. On the left, the corresponding moment rate functions. b) *SH* wave data (continuous line) and synthetic waveforms computed by *Pino et al.* [2000] for two different apparent source durations, derived from the *P* wave durations illustrated in Figure 10 and corresponding to southward and northward rupture propagation, respectively (HAM, Hamburg). From the better waveform correspondence and the consistency

of the seismic moment with those resulting for P waves, *Pino et al.* [2000] deduced that rupture propagation must have been dominantly northward.

**Figure 9.** Slip distribution along-strike of the fault resulting from various studies. The diagram consistently shows the maximum slip recorded along each section of the fault. The horizontal bars below the diagram mark the corresponding fault length and relative position along a N-S section. Dashed red lines represent the slip error resulting from the seismic moment uncertainty given in *Pino et al.* [2000].

**Figure 10.** Synoptic view of the 1908 earthquake rupture history and of the associated damage. The intensity pattern (from *Guidoboni et al.* [2007]) is shown with a color scale ranging from yellow to blue (intensity VI to XI, respectively); the area of strongest shaking is outlined by a dotted/dashed line (see also **Figure 1**). The black box is the surface projection of the model fault proposed by *Boschi et al.* [1989] (**E** in **Figure 7**). The star locates the epicenter proposed by *Michelini et al.* [2005b]. The black arrow indicates the rupture directivity proposed by *Pino et al.* [2000]. See text for discussion

**Figure 11.** Comparison between 1908 observed coseismic subsidence (above) and the elevation of the 125 ka terrace inner edge along the Calabria shore of the Messina Straits from Scilla (to the north; far left in figure) to Lazzàro (south; far right), suggesting that repeating 1908-type earthquakes may reproduce the young landscape of the region (from *Valensise and Pantosti* [1992]).

**Table 1.** Overview of the main accomplishments in the investigation of the source of the 1908 earthquake.

Year	Observation/Parameter	Value	Reference
<i>Early studies</i>			
1909	Elevation changes measured at 114 benchmarks on the two shores of the Straits	-0.64 m $\div$ + 0.13 m	Loperfido (Figure 4)
1909	Determination of epicentral area from direction of over-turned free-fall bodies	middle of the Straits	Omori (Figure 1a)
1909	Tsunami run-up height, period, and direction of approach measured at over 130 sites	up to 12 m	Platania (Figure 2)
1909	First mareogram recordings of a large tsunami in the Mediterranean	---	Platania (Figure 3)
1909	Hypocentral depth	9 km	Oddone
1910	Full macroseismic intensity pattern	---	Baratta (Figure 1b)
1954	First instrumental magnitude	7½	Gutenberg and Richter
<i>Modern studies (1970s-1990s)</i>			
1974	First focal mechanism from first motion polarities	strike 15°, dip=20°, rake=-90°	Ruscetti and Schick, Schick (1977) (Figure 6)
1977	First instrumental determination of epicenter	38.08 N 15.50 E	Schick
1977	First quantitative analysis of seismic waveforms	---	Schick
1983	First uniform slip elastic dislocation model of earthquake source	---	Mulargia and Boschi (Figure 7 B)
1983	First seismic moment estimate from geodetic data	2.0×10 <sup>19</sup> N m	Mulargia and Boschi
1983	First analytical model of tsunami source	---	Tinti and Giuliani
1989	First variable slip elastic dislocation model of earthquake source	---	Boschi et al. (Figure 7 E)
1992	Recurrence interval from long-term geological observations	1000 (+500, -300) years	Valensise and Pantosti (Figure 11)
1992	Long-term slip rate	1.4 mm/y	Valensise and Pantosti (Figure 11)
1995	Magnitude from intensity observations (equivalent magnitude M <sub>e</sub> )	7.2	Boschi et al. (CFTI catalogue)
<i>Most recent studies</i>			
1999	First comparison of tsunami patterns based on published source models	---	Tinti et al.
2000	First seismic moment $M_0$ (and moment magnitude $M_w$ ) from waveform modeling	5.8×10 <sup>19</sup> N m (7.1)	Pino et al. (Figure 8)
2000	Source-time function from waveform modeling	---	Pino et al. (Figure 9)
2000	Rupture directivity	from south to north	Pino et al. (Figure 10)
2000	Recurrence interval from archeological evidence	1,500 years	Guidoboni et al.
2002	Joint inversion of seismological and geodetic data	---	Amoruso et al. (Figure 7 G)
2004	Extension rate across the Messina Straits from GPS data	3 mm/y	D'Agostino and Selvaggi
2005	Probabilistic epicentral location from first arrivals	37.96 N 15.71 E	Michellini et al. (Figure 10)

**Table 1**

**Table 2.** Schematic overview of the main results obtained for the 1908 Messina Straits earthquake by several investigators, based on the analysis of instrumental, seismological and geodetic data (from *Pino et al.* [2000], modified and extended).

Author	$M_L$	$M_S$	$M_0$ , N×m	Fault plane	Fault ( $l \times w$ ), m <sup>2</sup>	Slip, m	Data type <sup>p</sup>
Gutenberg and Richter (1954)	7½	-	(9.4×10 <sup>19</sup> )	-	-	-	S
Kárník (1969)	7.0	-	(2.0×10 <sup>19</sup> )	-	-	-	S
Schick (1977)	7.1, 6.8, 7.1 <sup>d</sup>	7.0	(4.4×10 <sup>19</sup> )	15 20 -90 / 195 70 -90	30×15	1.50	S
Schick (1977)	-	-	5.0×10 <sup>18</sup> <sup>j</sup>	-	-	-	S
Schick (1977)	-	-	5.0×10 <sup>17</sup> <sup>k</sup>	-	-	-	S
Caputo (1980)	-	7.0	(4.4×10 <sup>19</sup> )	-	-	-	S
Caputo et al. (1981)	-	-	-	17 56 -97 / 209 34 -79	-	-	G
Abe (1981)	7.5 <sup>e</sup>	-	-	-	-	-	S
Abe (1981)	-	7.2	(8.7×10 <sup>19</sup> )	-	-	-	S
Gasparini et al. (1982)	-	-	-	349 42 -121 / 209 55 -65	-	-	S
Abe and Noguchi (1983)	-	7.0	(4.4×10 <sup>19</sup> )	-	-	-	S
Mulargia and Boschi (I) (1983) <sup>b</sup>	-	-	2.0×10 <sup>19</sup>	22 35 -90	20×12	1.50	G
Mulargia and Boschi (II) (1983) <sup>b</sup>	-	-	2.0×10 <sup>19</sup>	202 70 -90	20×16	1.50	G
Bottari et al. (1986)	7.3 <sup>f</sup>	-	(5.1×10 <sup>19</sup> )	-	-	-	M
Capuano et al. (1988)	6.9, 7.0, 7.2 <sup>g</sup>	7.1	(6.2×10 <sup>19</sup> )	same as Gasparini et al. (1982), from the same data	-	-	S
Capuano et al. (1988)	-	-	4.9×10 <sup>19</sup>	355 38.6 -132.5	56.7×18.5	1.50	G
Console and Favali (1988)	-	6.9 <sup>i</sup>	(3.1×10 <sup>19</sup> )	-	-	-	S
Hurtig and Kowalle (1988)	7.2 <sup>h</sup>	-	(3.8×10 <sup>19</sup> )	-	-	-	S
Boschi et al. (1989)	-	-	3.7×10 <sup>19</sup>	11 29 -90	45×18	1.42 <sup>m</sup>	G
De Natale and Pingue (1991)	-	-	3.5×10 <sup>19</sup> <sup>i</sup>	-	50×20	1.50 <sup>n</sup>	G
Boschi et al. (1995)	7.2 <sup>f</sup>	-	-	-	-	-	M
Pino et al. (2000)	-	-	5.8×10 <sup>19</sup>	-	43.3×20	2.07	S
Amoruso et al. (2002) <sup>c</sup>	-	-	2.4(6.0)×10 <sup>19</sup>	345.5 42.4 -118.3	29.8×19.8 (100×30)	-	G
Guidoboni et al. (2007)	7.1 <sup>f</sup>	-	-	-	-	-	M

<sup>a</sup> Seismic moment in parentheses are computed by using the formula derived by Ekström and Dziewonski (1988) for  $M_S$  to  $M_0$  and by Chung and Bernreuter (1981) for  $M_L$  to  $M_0$ . Except for Schick (1977) and Pino et al. (2000), all of the others are from geodetic data. Both nodal planes are reported for seismic data solutions, while single planes are relative to geodetic data.

<sup>b</sup> Fault planes I and II are relative to a single solution acting in a graben-like structure.

<sup>c</sup> Uniform slip inversion (values in parentheses are referred to variable slip inversion)

<sup>d</sup>  $m_B$  at Graz (GRZ), Wien (VIE), and Potsdam (POT), respectively.

<sup>e</sup>  $m_B$ .

<sup>f</sup> Macroseismic.

<sup>g</sup>  $m_B$  at Graz (GRZ), Sofia (SOF), and Zi-ka-wei (ZKW), respectively.

<sup>h</sup> At Potsdam (POT).

<sup>i</sup> At Rocca di Papa (RDP).

<sup>j</sup> From body waves at Hohenheim (HOH).

<sup>k</sup> From Rayleigh waves at Pulkovo (PUL).

<sup>l</sup> G. De Natale, personal communication.

<sup>m</sup> Constant slip. They also performed variable slip inversion.

<sup>n</sup> Average slip.

<sup>p</sup> S=seismometric, G=geodetic, M=macroseismic.

**Table 2**





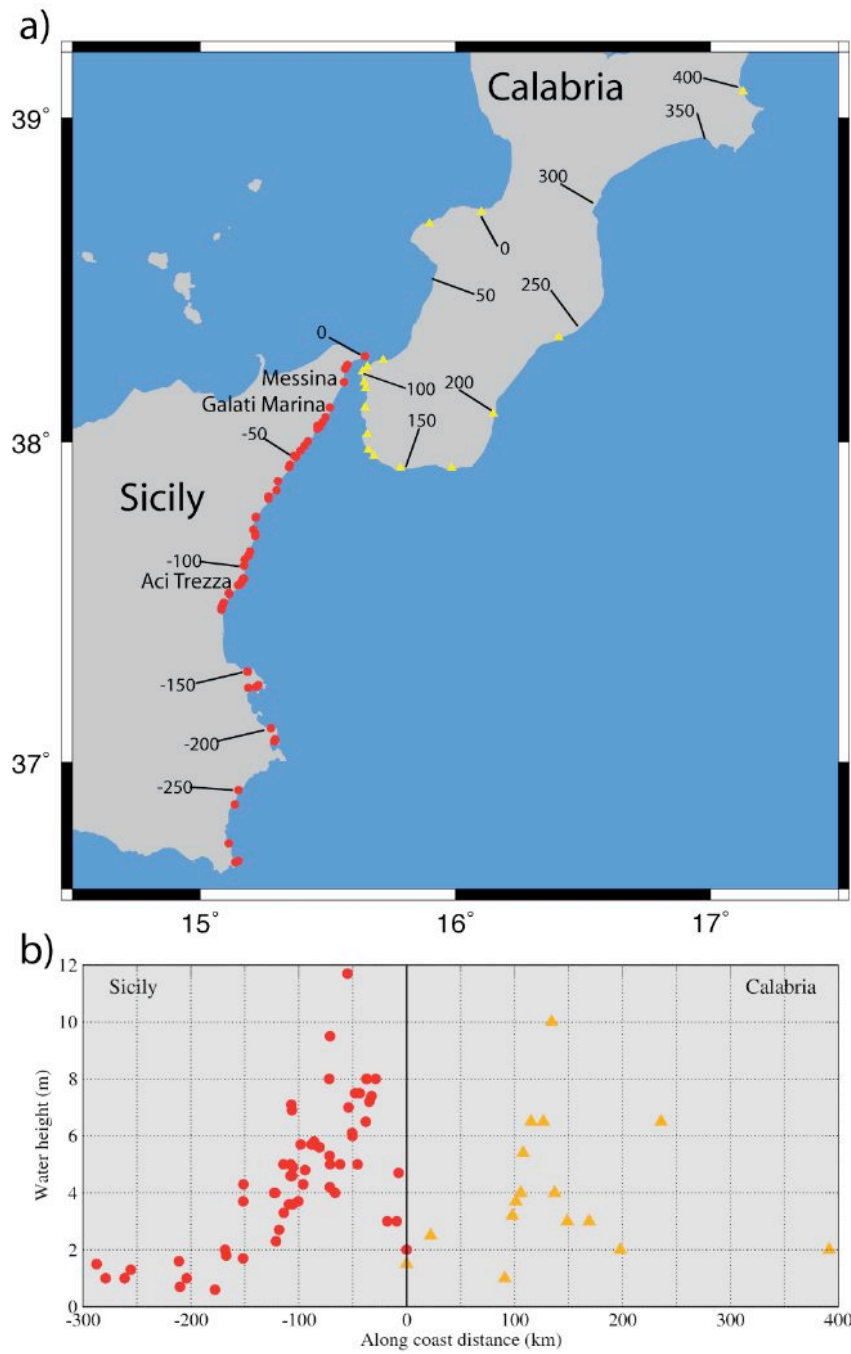


Figure 2

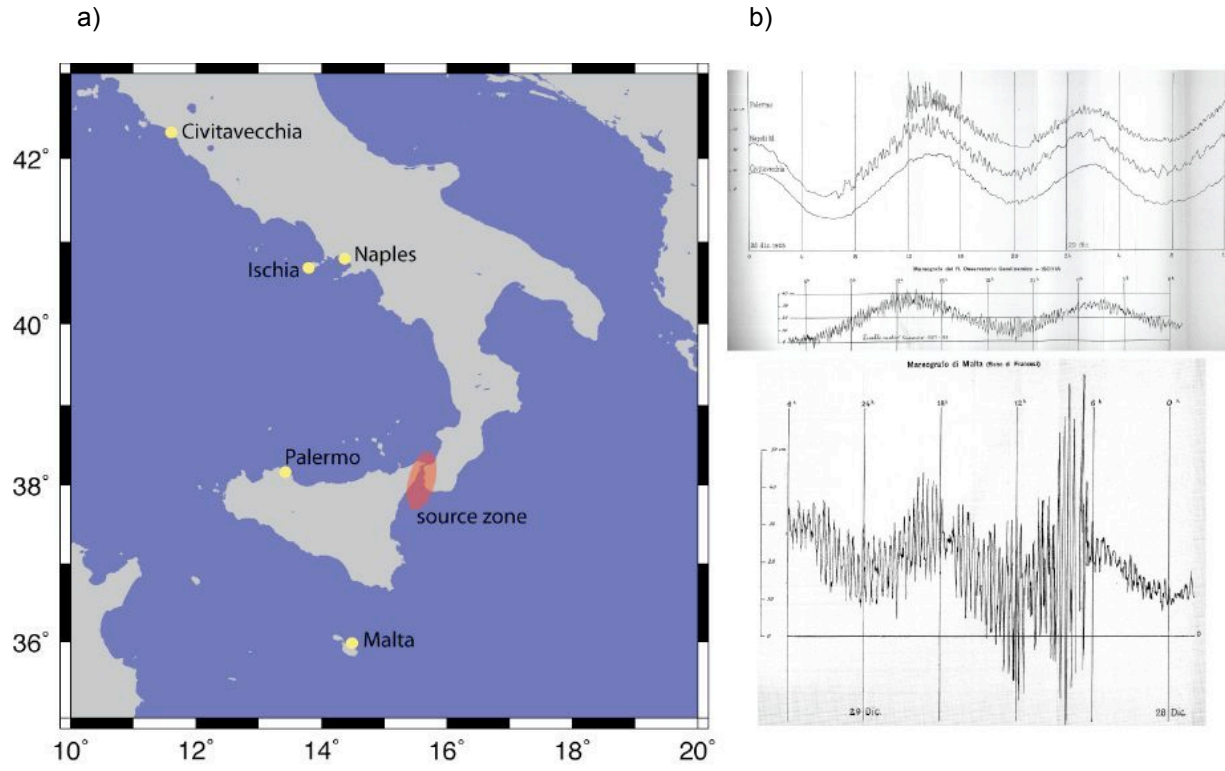


Figure 3

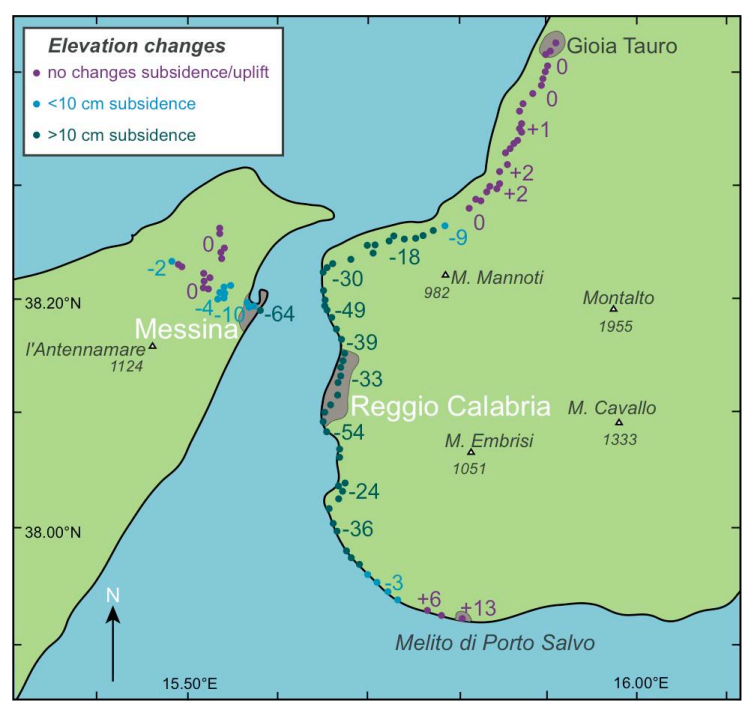


Figure 4

PLNn

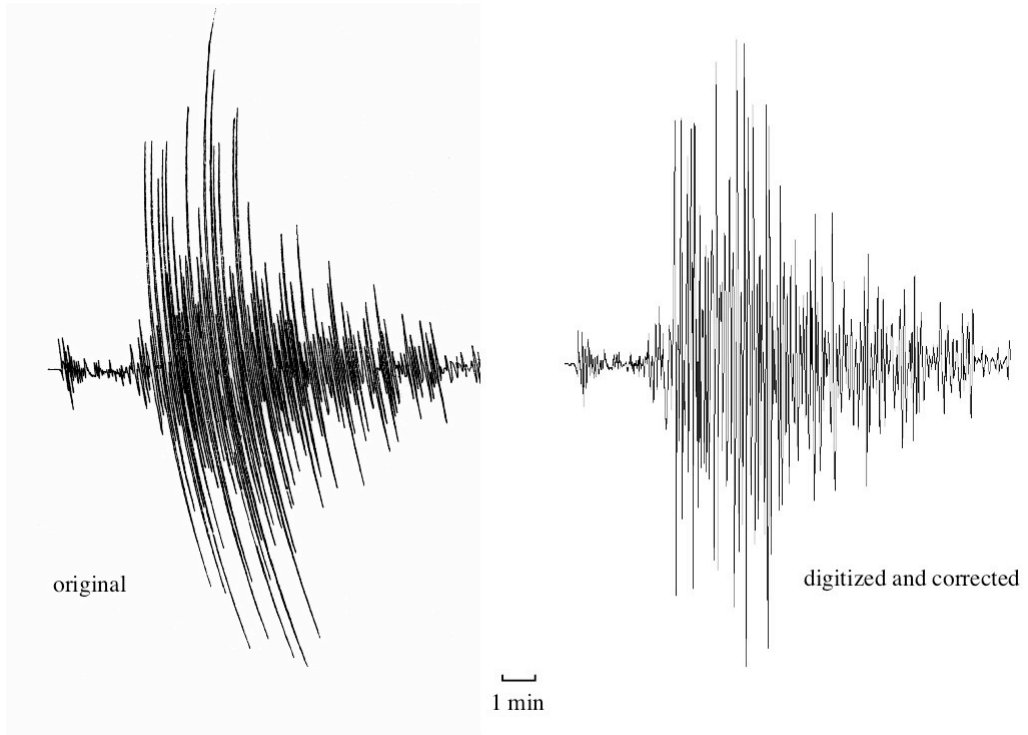


Figure 5

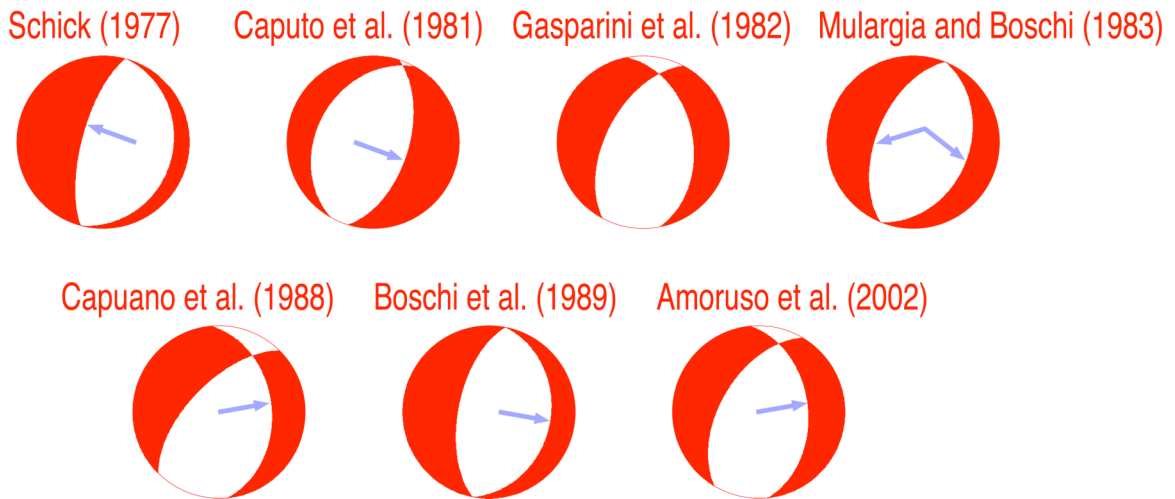


Figure 6

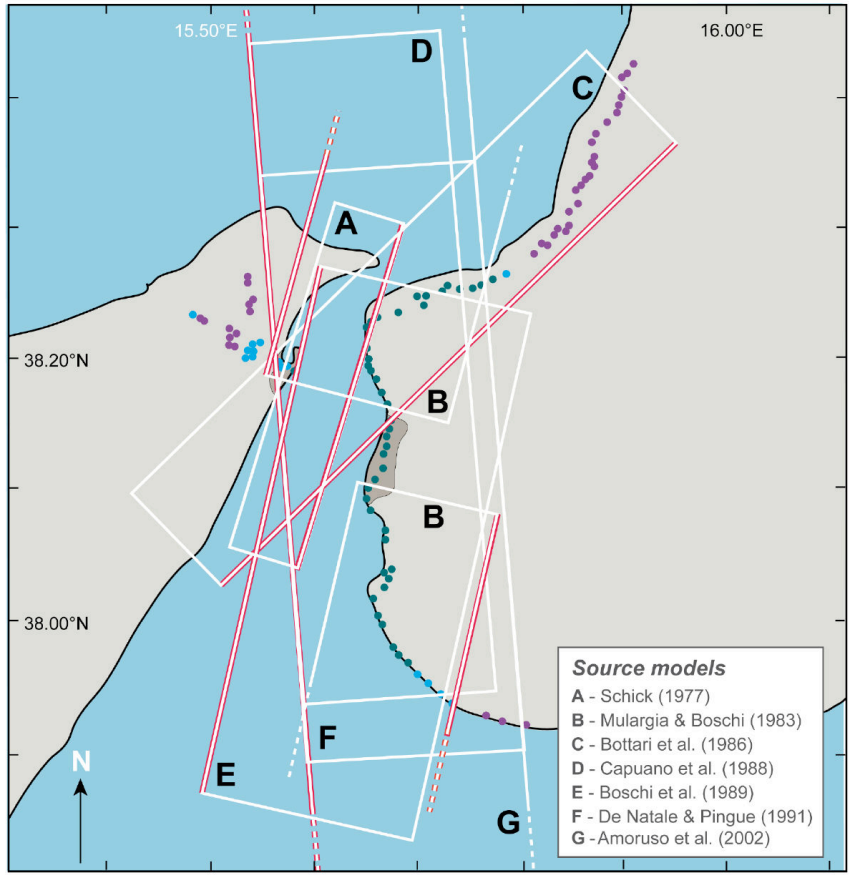
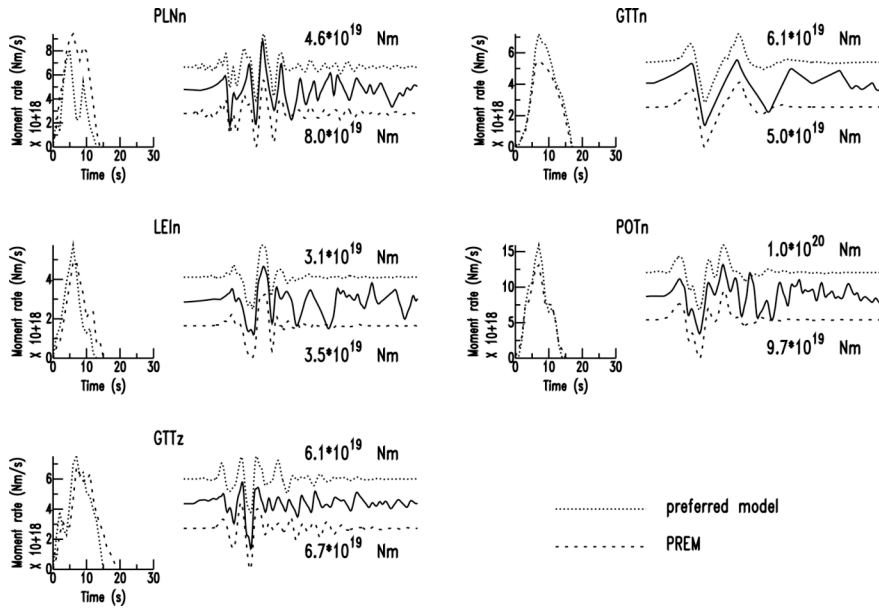


Figure 7

a)



b)

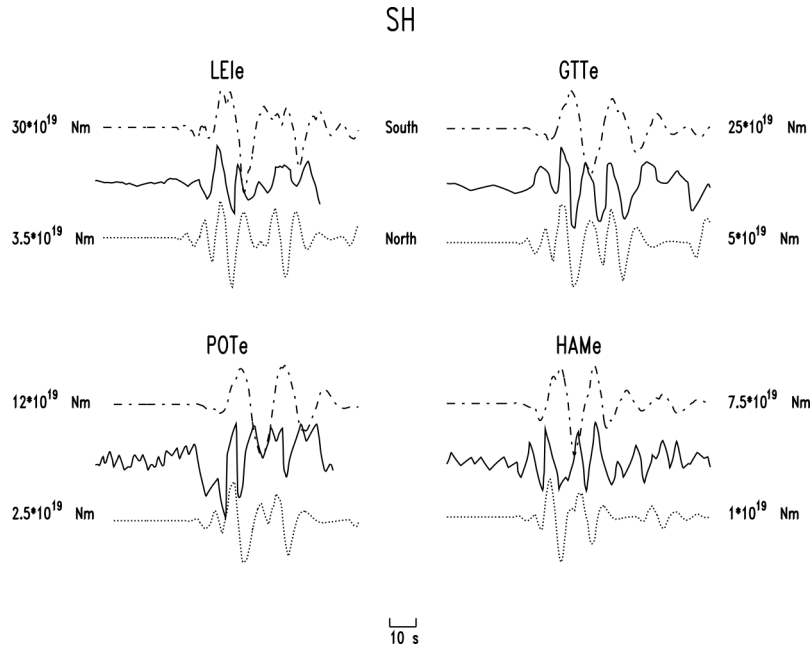


Figure 8

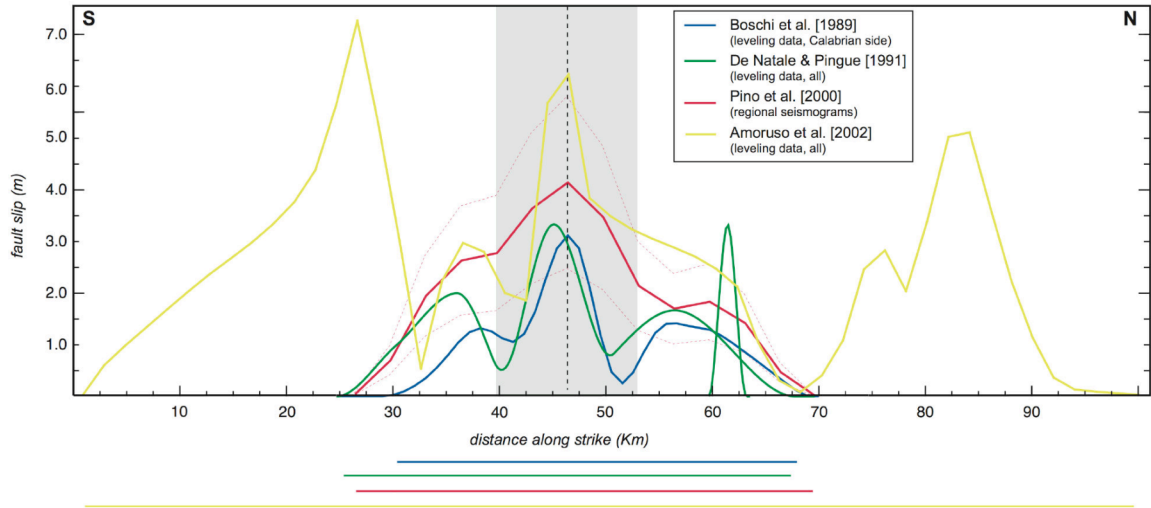


Figure 9

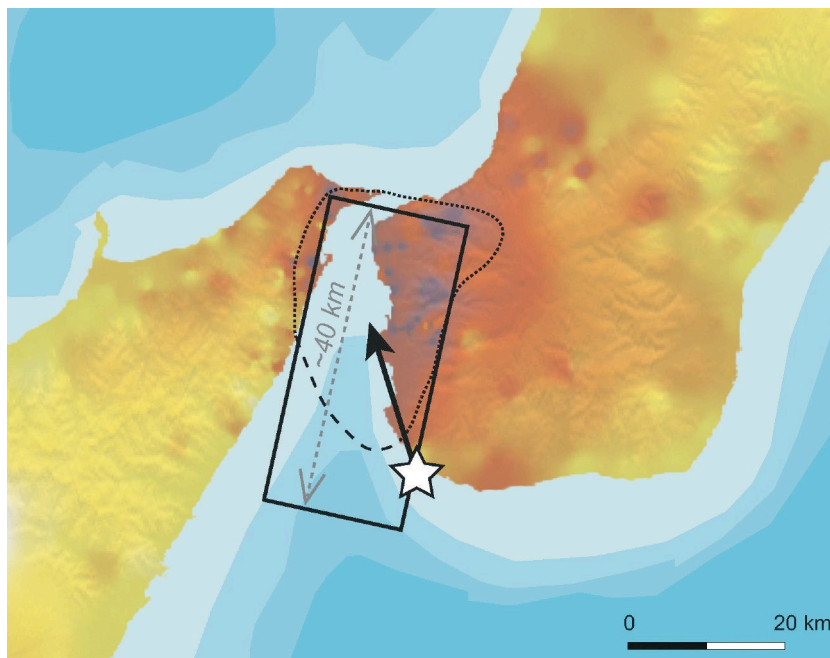
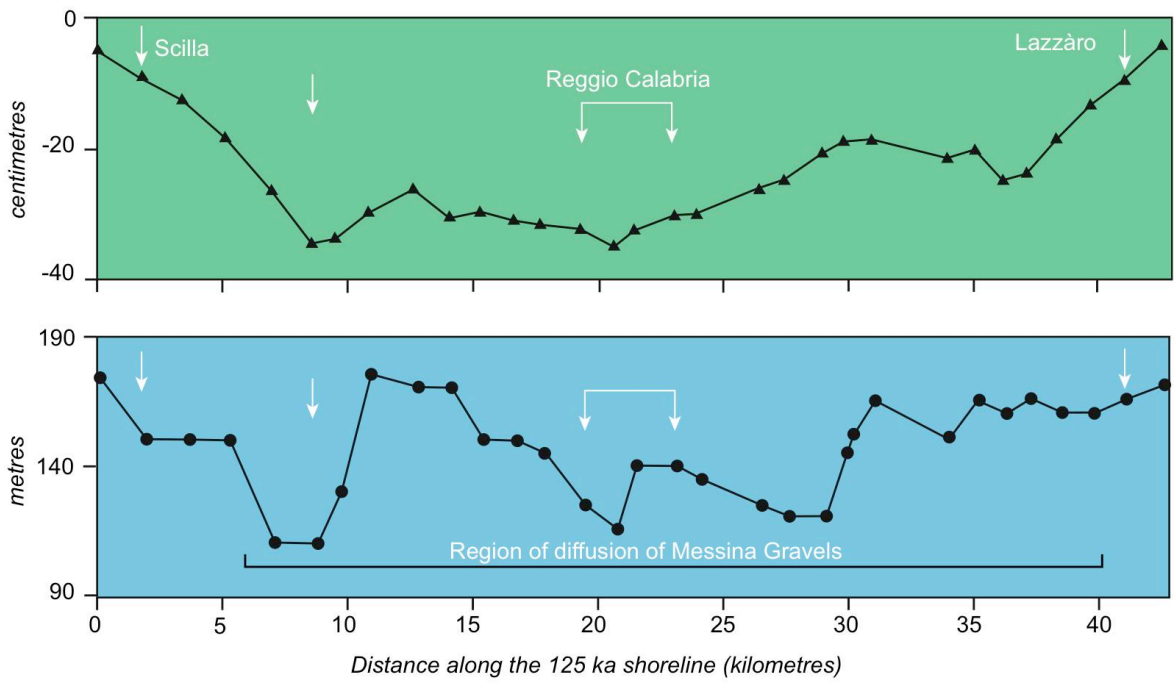


Figure 10



**Figure 11**